Journal of Chromatography B, 917–918 (2013) 53–61

Contents lists available at SciVerse ScienceDirect

Journal of Chromatography B

journal homepage: www.elsevier.com/locate/chromb

Identification and quantification of drug–albumin adducts in serum samples from a drug exposure study in mice

L. Switzar[a], L.M. Kwast[b], H. Lingeman[a], M. Giera[c,d], R.H.H. Pieters[b], W.M.A. Niessen[a,e,*]

[a] AIMMS Division of BioMolecular Analysis, Faculty of Sciences, VU University Amsterdam, De Boelelaan 1083, 1081 HV Amsterdam, The Netherlands
[b] Division of Toxicology, Institute for Risk Assessment Sciences, Utrecht University, PO Box 80177, 3508 TD Utrecht, The Netherlands
[c] Division of Molecular Cell Physiology, Faculty of Earth and Life Sciences, VU University Amsterdam, De Boelelaan 1085, 1081 HV Amsterdam, The Netherlands
[d] Biomolecular Mass Spectrometry Unit, Department of Parasitology, Leiden University Medical Center, Leiden, The Netherlands
[e] Hyphen MassSpec, de Wetstraat 8, 2332 XT Leiden, The Netherlands

ARTICLE INFO

Article history:
Received 12 September 2012
Accepted 10 December 2012
Available online 9 January 2013

Keywords:
Drug–protein adducts
Adverse drug reaction (ADR)
Serum albumin
NAPQI
Protein quantification
LC–MS(/MS)

ABSTRACT

The formation of drug–protein adducts following the bioactivation of drugs to reactive metabolites has been linked to adverse drug reactions (ADRs) and is a major complication in drug discovery and development. Identification and quantification of drug–protein adducts *in vivo* may lead to a better understanding of drug toxicity, but is challenging due to their low abundance in the complex biological samples. Human serum albumin (HSA) is a well-known target of reactive drug metabolites due to the free cysteine on position 34 and is often the first target to be investigated in covalent drug binding studies. Presented here is an optimized strategy for targeted analysis of low-level drug–albumin adducts in serum. This strategy is based on selective extraction of albumin from serum through affinity chromatography, efficient sample treatment and clean-up using gel filtration chromatography followed by tryptic digestion and LC–MS analysis. Quantification of the level of albumin modification was performed through a comparison of non-modified and drug-modified protein based on the relative peak area of the tryptic peptide containing the free cysteine residue. The analysis strategy was applied to serum samples resulting from a drug exposure experiment in mice, which was designed to study the effects of different acetaminophen (APAP) treatments on drug toxicity. APAP is bioactivated to *N*-acetyl-*p*-benzoquinoneimine (NAPQI) in both humans and mice and is known to bind to cysteine 34 (cys34) of HSA. Analysis of the mouse serum samples revealed the presence of extremely low-level NAPQI-albumin adducts of approximately 0.2% of the total mouse serum albumin (MSA), regardless of the length of drug exposure. Due to the targeted nature of the strategy, the NAPQI-adduct formation on cys34 could be confirmed while adducts to the second free cysteine on position 579 of MSA were not detected.

1. Introduction

Drugs that are associated with adverse drug reactions (ADRs) and idiosyncratic drug reactions (IDRs) frequently possess the propensity for bioactivation and subsequent formation of drug–protein adducts [1]. Although the exact mechanisms behind ADRs and IDRs still remain largely uncertain, drug–protein adducts are suggested to be directly linked to selective organ toxicity and immune-mediated response [2–4]. Elucidation of these mechanisms will lead to a better understanding of drug toxicity and may be achieved by identification of the target proteins of bioactivated drugs and their involvement in biological processes, such as inflammatory responses [1]. However, the detection of drug–protein adducts *in vivo* is extremely challenging since only minute amounts are present. Additionally, the low abundance of adducts in tissues and biofluids that possess a very wide dynamic range and a large excess of non-adducted proteins further complicates their detection. Therefore, sensitive and selective analytical methodologies are needed for the analysis of drug–protein adducts in complex biological samples.

Many target proteins of reactive drug metabolites have been identified from *in vitro* and *in vivo* animal experiments using global

Abbreviations: ACN, acetonitrile; ADR, adverse drug reaction; ALAT, alanine aminotransferase; APAP, acetaminophen; ASAT, aspartate aminotransferase; BSA, bovine serum albumin; cys34, cysteine on position 34; cys579, cysteine on position 579; DTT, dithiothreitol; EIC, extracted ion chromatogram; ESI+, positive-ion electrospray ionization; FA, formic acid; GHCl, guanidine HCl; HSA, human serum albumin; IAA, iodoacetic acid; IDR, idiosyncratic drug reaction; IS, internal standard; LC–MS, liquid chromatography mass spectrometry; MALDI, matrix-assisted laser desorption ionization; *m/z*, mass-to-charge ratio; MS, mass spectrometry; MSA, mouse serum albumin; MS/MS, tandem mass spectrometry; NAPQI, *N*-acetyl-*p*-benzoquinone imine.

* Corresponding author at: AIMMS Division of BioMolecular Analysis, Faculty of Sciences, VU University Amsterdam, De Boelelaan 1083, 1081 HV Amsterdam, The Netherlands. Tel.: +31 20 5987527.
E-mail addresses: w.m.a.niessen@vu.nl, mail@hyphenms.nl (W.M.A. Niessen).

1570-0232/$ – see front matter © 2013 Elsevier B.V. All rights reserved.
http://dx.doi.org/10.1016/j.jchromb.2012.12.033

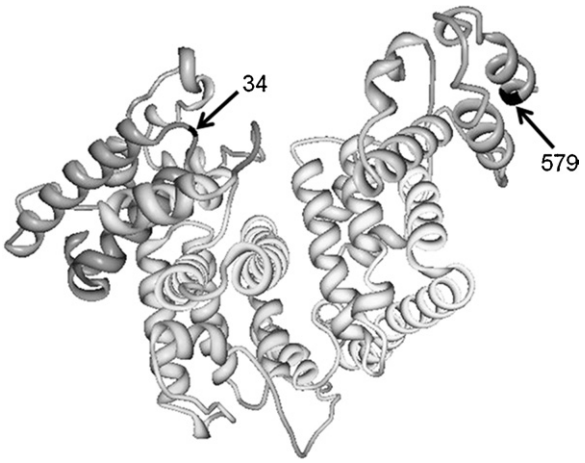

Fig. 1. Crystal structure of HSA (PDB ID: 2BXB [12], created with Protein workshop [13]) indicating the position of cys34 and location of residue 579, which is a cysteine in MSA.

proteomics approaches, such as two-dimensional gel electrophoresis in combination with mass spectrometry (MS) detection [5]. In such approaches, relevant protein spots are selected for further treatment based on autoradiography, in cases where radiolabeled drugs are used [6,7], or immuno-selective staining with antibodies raised against specific drugs [8,9]. The selected protein spots are excised from the gel, in-gel digested and analyzed with liquid chromatography mass spectrometry (LC–MS) [9] or matrix-assisted laser desorption ionization (MALDI)–MS [6–8]. Using immunoblotting, 15 hepatic proteins, 12 of which are novel, were identified recently as likely targets of tienilic acid in rats [9], while a total of 64 protein targets (42 cytosolic and 24 microsomal) of radiolabeled thiobenzamide were identified in rat liver using phosphorimaging [6]. Identification of the modification site, *e.g.*, *via* detection of an adducted peptide in a proteomics-based strategy, would unambiguously confirm adduct formation to the identified protein, but this is often not achieved due to the low level of covalent binding [10] and the small amount of protein present in the gel spot. Additionally, detection of the adducted peptide would provide a means for quantification of the level of adduct formation, which could have important clinical and toxicological relevance [5].

In vitro experiments using trapping agents have shown that numerous reactive drug metabolites are reactive toward the thiol group in cysteines [11] and many global proteomics approaches have identified human serum albumin (HSA) as a protein target for covalent binding [1]. This is due to the fact that HSA possesses an unpaired cysteine on position 34 (cys34) that is located on the surface of the protein and thus accessible to reactive drug metabolites, as can be seen in an image of the crystal structure (PDB ID: 2BXB [12], created with Protein workshop [13]) shown in Fig. 1. Using this information, a targeted approach can be developed to investigate covalent binding to HSA. Such a targeted approach includes selective protein isolation, *e.g.*, by affinity chromatography, prior to protein digestion and subsequent LC–MS analysis. This approach would provide the required selectivity and sensitivity for studying low-abundant proteins and their interactions [14,15]. The increased sensitivity of targeted approaches may also be useful for monitoring of drug–protein adducts in clinical samples [16] where radiolabels or other distinct features for selective detection are not applicable. A limited number of examples of a targeted approach for the confirmation of *in vivo* adduct formation have been reported for drugs [17,18] and other xenobiotic compounds [10]. In these studies, it was found that HSA, isolated from patient samples, was adducted at cys34 by nitrogen mustards [18] and *N*-acetyl-*p*-benzoquinoneimine (NAPQI), the reactive metabolite of acetaminophen (APAP) [17].

Covalent binding studies are an integral part of drug candidate evaluation in the pharmaceutical industry and may determine the fate of a lead compound. However, there is a need for advanced proteomics-based methodologies to study the relationship between drug–protein adducts and toxicity [19]. The NAPQI-albumin adduct is perhaps the most well-known example of drug–protein adduct formation and is therefore often used as a model adduct [20]. Drug toxicity studies are generally performed in animal models, thus it is fortunate that the protein sequence and structure, *i.e.*, disulfide bridges, of serum albumins are well conserved among various species [21,22]. Nevertheless, it is important to note that small differences in the protein sequence may lead to different binding effects [23]. Albumins of most species, including HSA and mouse serum albumin (MSA), contain the free cysteine on position 34. However, MSA represents a rather unique case because it also contains an additional free cysteine at position 579. Unfortunately, a crystal structure of MSA is not available, but, considering the fact that this cysteine is close to the C-terminus and the protein sequence is very similar to that of HSA, it is likely that this second free thiol in MSA is also accessible to reactive drug metabolites, see Fig. 1.

In the here presented research, an analytical strategy was developed and optimized for identification and quantification of low-abundant drug–albumin adducts. The optimized strategy was subsequently applied to serum samples resulting from a drug exposure study in mice. In this study, the mice received a dose of APAP either for a single day or for seven consecutive days in order to study the kinetics of ADRs and determine whether there is a correlation with the formation of NAPQI-MSA adducts.

2. Materials and methods

2.1. Chemicals and materials

Mouse serum albumin (MSA, ≥96%), bovine serum albumin (BSA, ≥98%), human serum albumin (HSA, 97–99%), acetaminophen (APAP, ≥99%), disodium hydrogen phosphate (Na_2HPO_4), sodium dihydrogen phosphate (NaH_2PO_4), potassium chloride (KCl), sodium chloride (NaCl), Bradford reagent, guanidine HCl (GHCl), ammonium bicarbonate (NH_4HCO_3), HPLC standard peptide mixture, [Met^5]Enkephalin acetate salt hydrate (≥95%, internal standard, IS), dithiothreitol (DTT), iodoacetic acid (IAA), *N*-acetyl-*p*-benzoquinone imine (NAPQI) and ethanol (96%) were obtained from Sigma Aldrich (Schnelldorf, Germany). A synthetic version of the HSA peptide ALVLIAFAQYLQQC$_{34}$PFEDHVK was kindly provided to us by R. Ekkebus (NKI, Amsterdam, The Netherlands). The HiTrap blue HP albumin affinity columns, prepacked with Blue Sepharose High Performance, (1 mL column volume) and NAP-25 gel filtration columns, prepacked with Sephadex G-25 DNA Grade, (2.5 mL column volume) were purchased from GE Healthcare (Diegem, Belgium). Trypsin from bovine pancreas (EC 3.4.21.4) was supplied by Roche (Almere, The Netherlands). LC–MS analyses were performed with ULC–MS grade acetonitrile (ACN, ≥99.95%) and formic acid (FA, 99%) from Biosolve (Valkenswaard, The Netherlands). Purified water was provided by a Millipore Milli-Q unit (Amsterdam, The Netherlands). For the mouse oral exposure experiments, APAP was dissolved in distilled water (Aqua B. Braun, Melsungen, Germany).

2.2. Mouse study design

Four to six weeks old female C3H/HeN mice were purchased from Harlan (Venlo, The Netherlands). Mice were specific

pathogen-free and maintained under barrier conditions in filter-topped macrolon cages with wood chip bedding at a mean temperature of 23 ± 2 °C, 50–55% relative humidity and a 12 h light/dark cycle. Drinking water and standard laboratory food pellets were provided *ad libitum.* The experiments were conducted according to the guidelines of, and with permission from, the animal experiments committee of Utrecht University. The C3H/HeN mice ($n = 8$) received either a single dose or seven consecutive daily doses of 300 mg/kg APAP. This dose was chosen using the maximum tolerable dose as described in the datasheet of the compounds and as used in previous experiments [24]. In both experiments, the control group consisted of eight mice that received the vehicle. The mice used in this study were part of a larger group ($n = 112$) that showed little variation in weight (mean weight ± SD of 21.25 ± 1.179 g). 17–24 h following the last oral dose, blood was drawn by cheek pouch puncture and both plasma and serum was collected (Minicollect, Kremsmünster, Austria) for further analysis. Furthermore, a part of the liver was isolated, fixed in formalin and subsequently embedded in paraffin.

Alanine aminotransferase (ALAT) and aspartate aminotransferase (ASAT) levels were analyzed in plasma samples on the AU400® Chemistry System (Beckman Coulter Nederland B.V., Woerden, The Netherlands) at NOTOX B.V. ('s-Hertogenbosch, The Netherlands). Plasma enzyme levels of APAP treated animals were compared to the combined control values obtained from both series of kinetics experiments. Multiple comparisons of group means were analyzed using one-way ANOVA with Dunnett's as post test. A value of $p < 0.05$ was considered significantly different compared to the control values. Data was analyzed using Graphpad Prism version 5.00 for Windows (Graphpad Software, San Diego, CA, USA).

2.3. Optimization of sample preparation protocol

The conditions of the albumin affinity chromatography, gel filtration chromatography and freeze-drying steps were optimized using standard serum albumin solutions with varying concentrations in various buffers. Initial experiments were performed with BSA or HSA; selected experiments were repeated with MSA. Recoveries were determined based on the Bradford assay quantification results, which were obtained as follows. A series of calibration solutions of 0–1.4 mg/mL were prepared of the albumin standard used in the specific optimization experiment and in the appropriate buffer. The readout was performed in 96-well plates in which 10 μL of sample or calibration standard was added to 200 μL Bradford reagent, in duplicate. The plates were incubated at room temperature for 15–45 min before readout in triplicate at 595 nm using a Victor^3 1420 Multilabel Counter plate reader from Perkin Elmer (Groningen, The Netherlands). The average absorbance of the triplicate measurements of the duplicate calibration samples was corrected for the blank and plotted against the concentration in mg/mL. The unknown protein concentrations of the samples were calculated using the linear regression equation obtained from the calibration curve.

LC–MS separation and detection conditions were optimized using a tryptic digest of standard MSA or NAPQI-MSA samples, prepared similarly as described in the next sections.

2.4. Preparation of mouse serum and MSA standard samples

Ideally, 50 μL of serum from each control ($n = 8$) and dosed ($n = 8$) mouse was used for analysis. In some cases, a smaller volume of serum was obtained and, therefore, all serum samples were weighed to determine the available volume. The ≤50 μL portions of mouse serum were adjusted to the composition of the HiTrap binding buffer by dilution with 950 μL of 20 mM $NaHPO_4$, pH 7.0. Additionally, a 10 μM reference standard of MSA in binding buffer ($n = 8$) was simultaneously prepared and received the same treatment as the serum samples.

Albumin was extracted from the mouse serum using HiTrap blue HP columns. The MSA reference standards underwent the same treatment in order to determine the recovery of MSA from the affinity column. The column was equilibrated with 10 column volumes of binding buffer followed by application of the sample. The unbound proteins were removed by washing the column with 10 column volumes of binding buffer. The bound MSA was eluted with 10 mL of elution buffer, consisting of 20 mM $NaHPO_4$, 2.0 M NaCl, pH 7.0. The first 3 mL of the elution step, containing the bulk of the bound MSA, was collected and used for further treatment. The total protein content was determined by Bradford assay as described in the previous section.

The purified MSA was buffer exchanged to denaturation buffer (2.0 M GHCl, 50 mM NH_4HCO_3, pH 8.5) using NAP-25 gel filtration columns. An improved protocol was used to avoid further dilution of the sample while maintaining a high recovery. The columns were equilibrated with 25 mL of denaturation buffer before application of the 3 mL sample. The protein fraction was subsequently eluted by application of an equal volume (3 mL) of the same buffer thereby avoiding dilution of the sample. The samples were allowed to denature overnight at 4 °C.

The following morning, the disulfide bridges in the MSA samples were reduced by the addition of a 50-fold molar excess (50 × total number of cysteines (36) × MSA concentration) of DTT and incubation at 50 °C for 30 min. After reduction, the samples were allowed to cool down to room temperature and the resulting thiol-groups were alkylated with a 75-fold molar excess of IAA (1.5-fold excess over DTT) at room temperature and in the dark for 30 min. Subsequently, a buffer exchange and desalting step was performed using the same NAP-25 protocol mentioned above, only now Milli-Q water was used for equilibration of the column and elution of the protein.

The samples were concentrated by freeze-drying for 6.5 h using a Centrivap concentrator (Labconco, Kansas City, MO, USA), which was kept at room temperature and was connected to an automatic freeze dryer (The VirTis Company Inc, Gardiner, NY, USA). The dried protein samples were either stored at −20 °C until further treatment or directly redissolved in 250 μL of 50 mM NH_4HCO_3 buffer, pH 8.4, followed by digestion. Tryptic digestion was performed overnight using optimized conditions as described elsewhere [25]. In short, trypsin was added to the samples in a protein-to-enzyme ratio of 100:1 (w/w). The samples were subsequently incubated at 24 °C overnight (∼15 h) followed by the addition of FA to a final concentration of 0.1%. Finally, the IS was added to a final concentration of 31.5 μM and a final volume of 350 μL was obtained by the addition of digestion buffer. The samples were either analyzed immediately with LC–MS or stored at −20 °C.

2.5. In vitro preparation of NAPQI-MSA adducts

To assess whether the cysteine 579 (cys579) residue in MSA is accessible to reactive drug metabolites and whether adduct formation can take place at this site, the NAPQI-MSA adduct was prepared *in vitro* according to the following protocol. Synthetic NAPQI (1 mg) was dissolved in 80 μL of DMSO and 30 μL of this solution, representing a 50-fold molar excess, was added to 3 mg of MSA reconstituted in 2.97 mL of a 10 mM PBS buffer, pH 7.4. The adduct formation reaction was left to proceed at room temperature for 1 h before buffer exchange to PBS buffer. Five sequential gel filtration steps were performed in order to completely remove the excess NAPQI and prevent adduct formation to other cysteines after reduction of the disulfide bridges. From then on, the purified

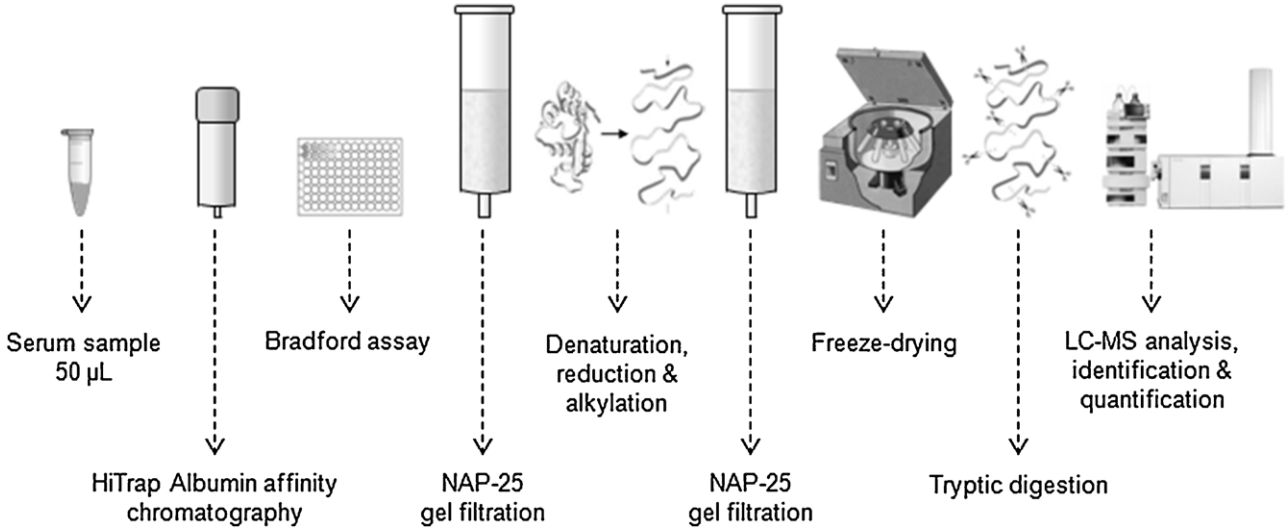

Fig. 2. Sample preparation and analysis strategy.

NAPQI-MSA received the same treatment as the mouse serum samples and was analyzed in triplicate.

2.6. LC–MS analysis

The digested MSA samples were analyzed with a 1200 series Rapid Resolution LC system coupled to a 6520 QTOF mass spectrometer (Agilent Technologies, Amstelveen, The Netherlands), that was controlled by the Agilent Masshunter Workstation Acquisition software (version B.02.00). The tryptic peptides were separated on an Agilent XDB-C18 column (50 mm × 4.6 mm, 1.8 μm particles) that was protected by a C18 guard column (4 mm × 2 mm) from Phenomenex (Utrecht, The Netherlands). The LC–MS settings were based on a previously published method for the analysis of NAPQI-HSA digests [25] and slightly modified for NAPQI-MSA digests. In order to gain additional retention for the cys34 and cys579 peptides, the mobile phases were changed to 2.5% ACN, 0.1% FA in water for eluent A and 2.5% water, 0.1% FA in ACN for eluent B. In addition, the gradient method was extended to a total runtime of 48 min. Gradient elution was performed by holding the % B at 0% for the first 5 min, followed by a linear increase to 40% B in 23 min. The column was then washed at 100% B for 7 min and re-equilibrated for the next run at 0% B for 13 min. The flow rate was set to 0.6 mL/min and the temperature of the thermostated column compartment was maintained at 40 °C.

Using an internal switch valve, the LC flow from 4 to 28 min was directed to the mass spectrometer, which was operated in 2 GHz, extended dynamic range mode. The electrospray ionization source was operated in positive mode (ESI+), the capillary voltage was set to 3500 V and nitrogen (99.9990%) was used as the drying (350 °C) and nebulizer gas at a flow rate of 12 L/min and a pressure of 60 psig, respectively. Profile data was acquired at a rate of 1.25 spectra/s in data-dependent mode where the most intense ion (m/z 300–2000) was selected for fragmentation and subsequently excluded from fragmentation for 0.2 min. Fragmentation spectra of selected ions were recorded over an m/z range from 50 to 2000, at a rate of 1.03 spectra/s using a fixed collision energy voltage of 20 V and nitrogen as the collision gas. An aqueous blank sample and the HPLC peptide standard mixture (containing 0.5 μg/mL of Gly-Tyr, Val-Tyr-Val, Met-enkephalin acetate, Leu-enkephalin and angiotensin II acetate) were analyzed after every sample run to check the stability of the LC–MS system throughout the sequence. These control samples were analyzed using a shorter method with a runtime of 22 min. During this method, the concentration B increased from 0 to 50% over the first 7 min, was held constant at 100% B for 5 min, and finally held at 0% B for 10 min. Full-spectrum MS data (m/z 200–1500) was collected during the first 7 min of the run at a rate of 1.03 spectra/s. The LC flow rate and ESI source conditions were the same as described above.

2.7. Data analysis

Peak extraction (using a 20 ppm half-width m/z window) and integration was performed with the Agilent Masshunter Qualitative Analysis software (version B.02.00). The peak areas were normalized to the peak area of the IS. The level of adduct formation was determined by the ratio between the peak area of the NAPQI-cys peptide divided by the total peak area of cys peptide (sum of all charge states of the carboxymethylated and NAPQI-modified).

3. Results and discussion

3.1. Method development and optimization

Albumin is the most abundant serum protein, but only a very small percentage is modified by reactive drug metabolites. This means that in our mouse study the NAPQI-MSA adduct is extremely low abundant and, adding to this challenge, it is in the presence of a large excess of non-modified MSA. Furthermore, the NAPQI-modification represents a very small addition of only 149.07 Da to the large MSA protein molecule of 65.9 kDa and does not have a large effect on the protein characteristics. The difference between the two MSA species is, therefore, too small to achieve a separation using conventional techniques. For the analysis of NAPQI-MSA adducts in serum, a sample preparation and analysis methodology was developed and optimized in order to deal with the low abundance of the NAPQI-MSA adduct (Fig. 2). The optimization of the various steps is discussed in some detail below.

The albumin, both NAPQI- and non-modified, was extracted from the mouse serum by albumin affinity chromatography using HiTrap cartridges. If available, a starting sample volume of 50 μL mouse serum was used that was adjusted to the HiTrap binding conditions by dilution with binding buffer. To determine the optimal dilution volume, different sample volumes of 1.0–3.0 mL were evaluated, but significant differences in the recovery of BSA were not detected (69 ± 8%, $n = 8$). An application volume of 1.0 mL (recovery 71 ± 11%, $n = 4$) was chosen for use in the final protocol. Regarding the elution volume, the bulk of HSA (> 90%) eluted within

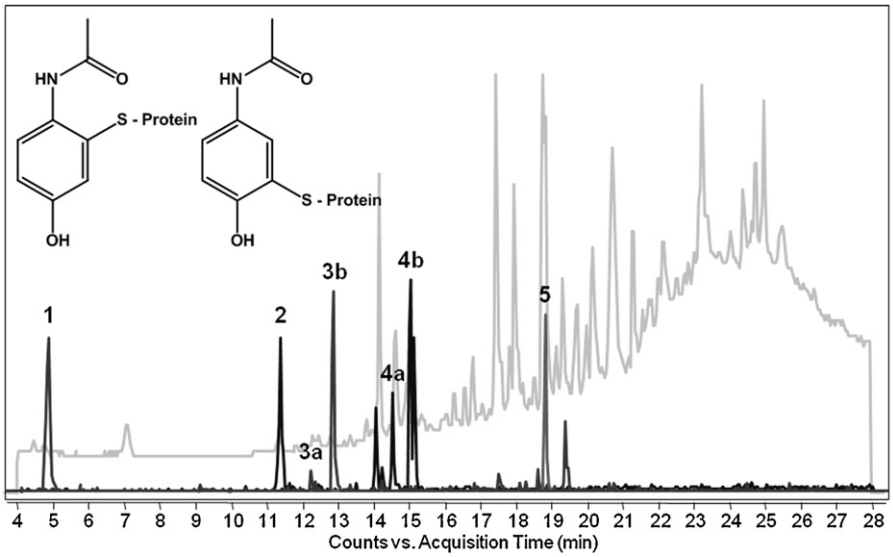

Fig. 3. LC–MS results from the analysis of a tryptic digest of NAPQI-MSA. The extracted-ion chromatograms (EICs) of the doubly charged ions with *m*/*z* 505.69 (peak 1, C_{34}(carboxymethyl)SYDEHAK), *m*/*z* 339.66 (peak 2, C_{579}(carboxymethyl)KDALA), *m*/*z* 551.23 (peaks 3a and b, C_{34}(NAPQI)SYDEHAK) and *m*/*z* 385.19 (peaks 4a and b, C_{579}(NAPQI)KDALA) are shown in black. In the background, a total ion chromatogram (TIC) is shown in gray. For purpose of clarity, different scales were used for the *y*-axis. Proposed structures of the regioisomeric adducts are shown in the top left corner.

the first 3.0 mL from the HiTrap cartridge, thus this was considered as the optimum elution volume. Finally, a different buffer system based on GHCl and NH_4HCO_3 at pH 8.5 was also investigated for HiTrap binding and elution, but this led to a decreased recovery of < 50%.

The recovery of BSA and HSA from the HiTrap columns using the standard $NaHPO_4$ binding and elution buffers at pH 7.0 was comparable, 87% and 90% ($n = 4$), respectively. However, the recovery decreased over time with repetitive use of the columns. Therefore, new HiTrap columns were used for the mouse serum samples. Unfortunately, the binding of MSA to the HiTrap columns is less efficient [26], resulting in a recovery of 59 ± 9% ($n = 16$). The low recovery could easily be compensated by increasing the initial starting volume of 25–50 μL serum, when available. Although this also leads to a higher concentration of non-modified MSA in the final sample, the final concentration of NAPQI-MSA will theoretically be in the nanomolar range (after the freeze-drying step), assuming that ~0.1% of the total MSA is modified by NAPQI. This concentration of NAPQI-MSA is well within the detectable range.

The HiTrap albumin affinity step leads to a 60-fold dilution of the original 50 μL of serum to 3 mL of purified albumin. To avoid further dilution and sample losses, the standard NAP-25 gel filtration protocol (application of 2.5 ml of sample and elution with 3.5 ml buffer) was adapted for better alignment with the HiTrap elution step. Therefore, the total 3.0 mL of eluted sample from the HiTrap cartridges was applied to the gel filtration column and elution from this column was performed with 3.0 mL of buffer. Using a 1 mg/mL BSA solution in water, the recovery of this protocol was found to be above 90% and with two consecutive gel filtration steps the recovery was still above 85%. In order to counteract the 60-fold dilution and increase sensitivity, the effect of a freeze-drying step on protein stability and recovery was also investigated. After 6-h of freeze-drying and redissolving the dried protein in a volume of 250 μL, a more than 10-fold concentration factor and a recovery of 94 ± 6% ($n = 6$) were achieved.

The tryptic digestion and LC–MS conditions were optimized previously for NAPQI-HSA cys34 adducts with respect to protein coverage and peak area of the modified cys34 peptide [25]. These optimized conditions also provided better results in the identification of MSA adducts and, thus, were applied in the current study. However, the peptides of interest containing the possible adduct formation sites resulting from the tryptic digestion of (NAPQI-)MSA, C_{34}SYDEHAK and C_{579}KDALA, are much shorter in length than the cys34 peptide of HSA, ALVLIAFAQYLQQC_{34}PFEDHVK. The cys579 peptide still contains a lysine, but this is not considered as a tryptic cleavage site due to the cysteine in the p2 position and aspartic acid in p1', as is stated for the tryptic cleavage rules in the ExPASy database [27]. This part of the MSA sequence was also never detected in any other form. The relatively short carboxymethylated cys34 and 579 peptides from MSA showed little retention and co-eluted with the IS. Therefore, some adjustments to the LC–MS method were made for increased retention and separation of the peptides of interest. Additionally, several peptides were tested for use as an IS; Met-Enkephalin (YGGFM) was selected due to its favorable retention time of 18.8 min (peak 5). With this optimized method, the C_{34}(carboxymethyl)SYDEHAK (peak 1, t_R 4.9 min) and C_{579}(carboxymethyl)KDALA (peak 2, t_R 11.4 min) could be separated and detected, see Fig. 3 Furthermore, two peaks were observed for each NAPQI-cys peptide adduct, which is most likely due to the formation of regioisomers [17], see peaks 3 and 4, a and b in Fig. 3.

3.2. Adduct quantification

Information about the level of albumin adduct formation present in the mouse serum is necessary in order to determine the effect of different drug exposure regimes in the two mouse studies. Ideally, quantification of the NAPQI-MSA adduct in the samples would be done at the protein level. However, since the resolution between MSA and NAPQI-MSA and/or the sensitivity were simply insufficient in MALDI–ToF MS and Orbitrap MS experiments (data not shown), quantification could only be done at the peptide level where the NAPQI-modified peptides are easily separated from the non-modified species.

In order to achieve reliable quantification, an internal standard must be used [28]. Given the large sequence homology between albumins, a tryptic cys34 or cys579 peptide from another albumin with a slightly different sequence would be a good choice. Unfortunately, MSA is the only commercially available albumin with a free cys579 and yields a much shorter cys34 peptide than other

albumin species. Another possibility would be absolute adduct quantification using a synthetically prepared NAPQI-cys34 peptide, as applied by Damsten et al. [17]. Using a synthetic NAPQI-cys34 peptide, levels of 3–35 pmol/mL of NAPQI-HSA adducts in patient serum were detected. However, this approach requires a labeled reference peptide to be synthesized for each adduct, which can be a tedious process. An extra limitation for the preparation of reference adducts is the limited availability of reactive metabolites since NAPQI is the only one that can be obtained commercially.

Another evaluated option was the use of a MSA reference standard for external quantification of the NAPQI-MSA level in the mouse serum samples. This was accomplished by comparing the peak areas of five selected MSA peptides to the peak areas of the corresponding peptides in the tryptic digests of the purified mouse serum samples. This provides the total MSA concentration. Subsequently, a decrease in the peak areas of the non-adducted cys34 and 579 peptides in both types of samples can be assumed to be a measure of the percentage of NAPQI-modified MSA in the mouse serum samples. The five reference peptides were selected from the MSA digest based on the following criteria: (1) not to contain cysteines in order to prevent problems with incomplete reduction and alkylation, (2) be well distributed over the chromatogram and the protein sequence, (3) no missed cleavages in or next to peptide in order to prevent inaccuracies due to incomplete digestion, (4) limited coelution with other peptides. All peptides were normalized to the IS to correct for changes of MS signal intensity over time. Using this strategy, the MSA concentration in the *in vitro* generated NAPQI-MSA samples could be determined accurately at 84 ± 14% of the actual concentration (n = 5 or 7). The adduct levels were predicted to be 40 ± 3% and 51 ± 13% for cys34 and 579, respectively. Unfortunately, when this strategy was applied to the serum samples from the mouse study, it suffered from matrix effects most likely caused by the co-extraction of other serum proteins during the albumin affinity chromatography step and the biological variation. These phenomena result in high %RSD values making it problematic to accurately quantify adduct levels of 0.1%.

Finally, it was decided to perform a relative quantification of the NAPQI-MSA adduct level within each sample without the use of any reference standard, thereby avoiding all disadvantages described above. This was done by determination of the relative ratio between the peak areas of all charge states of the NAPQI-cys peptide and that of the total cys peptide peak area, which is the sum of the NAPQI-cys and carboxymethylated-cys peptide. Hereby, it was assumed that the ionization efficiency of both forms of the cys peptides was similar. With this method, all samples could be subjected to quantification under the same conditions and low adduct levels could be determined.

3.3. Analysis of in vitro NAPQI-MSA

In contrast to HSA, MSA contains a second free cysteine at position 579. No information was available about the accessibility of this cysteine for small molecules. By *in vitro* incubations of MSA with synthetic NAPQI under non-denaturing conditions, it was shown that cys579 can also be modified with NAPQI (synthetic labeling efficiency 79 ± 1.3%), even to a higher extent than cys34 (55 ± 2.5%). If this adduct is also found *in vivo*, it could have implications for the extrapolation of drug toxicity effects in mice to human. For both the C_{34}(NAPQI)SYDEHAK and C_{579}(NAPQI)KDALA peptides, the formation of the later eluting regioisomer is strongly favored over the other. Sequence analysis of the MS/MS spectra of the ions m/z 505.69 (t_R 4.9 min, C_{34}(carboxymethyl)SYDEHAK) and m/z 551.23 (t_R 12.9 min, C_{34}(NAPQI)SYDEHAK), shown in Fig. 4A and B, confirms the presence of the NAPQI adduct on the cys34 position by the presence of an almost complete y-ion sequence. Characteristic ions of the doubly (m/z 551.23) and triply charged (m/z 367.83) C_{34}(NAPQI)SYDEHAK peptide of the other regioisomer (t_R 12.1 min) were observed, their intensity was insufficient for adequate MS/MS fragmentation. Due to the short length of the cys579 peptide, the MS/MS spectra of the C_{579}(carboxymethyl)KDALA (t_R 11.4 min, Fig. 4C) and C_{579}(NAPQI)KDALA (t_R 15.0 min, Fig. 4D) are more challenging to interpret, but the presence of the NAPQI-cys adduct on position 579 could be confirmed from a partial b-ion sequence. The identification of the C_{579}(NAPQI)KDALA peptides is further complicated by the adjacent elution of isobaric peptides (m/z 385.21, t_R 14.1 and 15.2 min) with the same charge state. However, the MS/MS spectra of these ions contain a fragment ion with m/z 147.11 characteristic of a C-terminal lysine (data not shown) and, thus, are distinctly different peptides.

3.4. Histological and liver enzyme analysis

Hepatoxicity caused by oral exposure to APAP was determined by both histological analysis and plasma levels of the liver enzymes ALAT and ASAT. Blood flow in the liver runs from the portal area toward the central veins from which blood is subsequently transported to the inferior vena cava. Previous animal experiments showed that administration of APAP resulted in liver damage, indicated by the presence of necrotic areas around the central vein areas [29–32]. Histological examination of the mouse livers from the current study showed similar necrotic centrilobular areas in the livers from mice orally exposed to APAP, which could be identified by minor cell swelling and loss of hepatic structure at this site, see Fig. 5. Surprisingly, no clear differences in liver damage and necrotic areas were observed between the groups that received a single or seven consecutive exposures to APAP.

In addition to the histological analysis, serum levels of the liver enzymes ALAT and ASAT were determined, see Fig. 6 for the resulting bar graphs. Serum biomarkers, such as ALAT and ASAT levels, are generally used to indicate the presence of liver injury following drug exposure [32–34]. In our experiments, the level of ALAT in plasma was significantly increased in both the single and seven times exposed groups, which is indicative for APAP-induced liver damage. However, this effect was not observed for ASAT levels. Similar to the histological analysis, also no differences were observed between the single and multiple dosed groups in terms of liver enzymes. Several experiments have shown time dependent increases in liver enzyme levels following administration of APAP. However, there does not seem to be a clear relationship between ALAT en ASAT levels, as exemplified by several studies performed in animals [35,36] and humans [17,37].

3.5. Analysis of NAPQI-MSA in mouse serum samples

Finally, the optimized analysis and quantification strategy was applied to the serum samples from the mouse study. The one- and seven-day experiment each consisted of eight control mice and the same number of dosed mice, resulting in the collection of 16 serum samples for each experiment. Low-abundant NAPQI-MSA adducts to cys34 were detected in all of the serum samples collected from the dosed mice, of both the one-day and seven-day experiment, see Fig. 7. In the extracted ion chromatogram (EIC) of triply charged C_{34}(NAPQI)SYDEHAK (m/z 367.82 at 12.7 min, Fig. 7A), a significant difference was observed between the control and dosed mouse serum sample. The other regioisomer of C_{34}(NAPQI)SYDEHAK is also present at 12.1 min, albeit at a very low intensity. No difference was observed between control and dosed mice in the EICs of m/z 385.19, the expected m/z of the doubly charged C_{579}(NAPQI)KDALA (Fig. 7B). Although the cys579 residue could be modified by NAPQI *in vitro*, this adduct was not detected *in vivo*. Reasons for this could be a preference for modification of cys34 by NAPQI *in vivo*, resulting in a lower modification level of cys579 and possibly insufficient

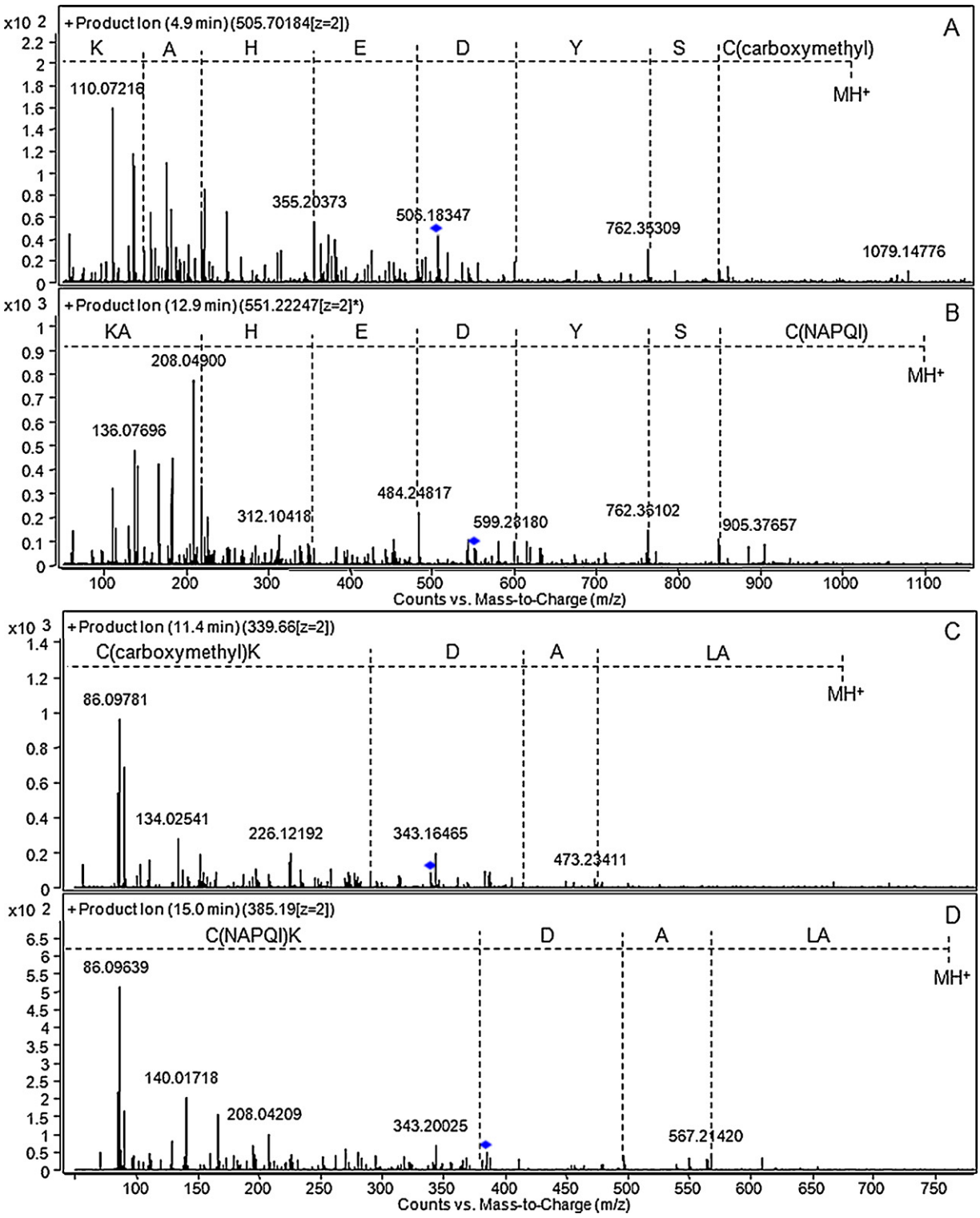

Fig. 4. MS/MS spectra of C_{34}(carboxymethyl)SYDEHAK (A), C_{34}(NAPQI)SYDEHAK (B), C_{579}(carboxymethyl)KDALA (C) and C_{579}(NAPQI)KDALA (D).

abundance for detection, or a complete absence of cys579 modification.

The total MSA concentration in the final sample and in serum was calculated based on the results of the Bradford assay and the empirically established recoveries of MS after each of the sample preparation steps, see Table 1. Liver toxicity is the ADR associated with APAP overdose and changes in the serum albumin level could be a first indication of a disruption in liver function. However, the albumin levels in the APAP-dosed mice were not different from those of the control mice, nor were there significant differences detected between the one- and seven-day experiments.

By application of the relative quantification strategy based on the tryptic cys34 peptides, the NAPQI-MSA adduct levels detected in the dosed mouse serum samples of both the one- and seven-day

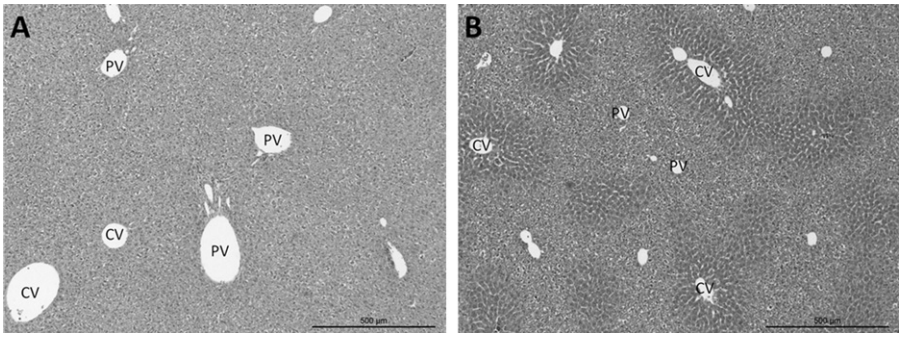

Fig. 5. Histological representation of liver. Mice were exposed orally to either a single or seven consecutive doses of acetaminophen. Within 24 h of the last dose, a part of the liver was collected and paraffin embedded sections of the liver were stained with hematoxylin and eosin. Representative sections for controls (A) and APAP (B) treated animals are shown. PV: portal vein, CV: central vein (magnification 4×).

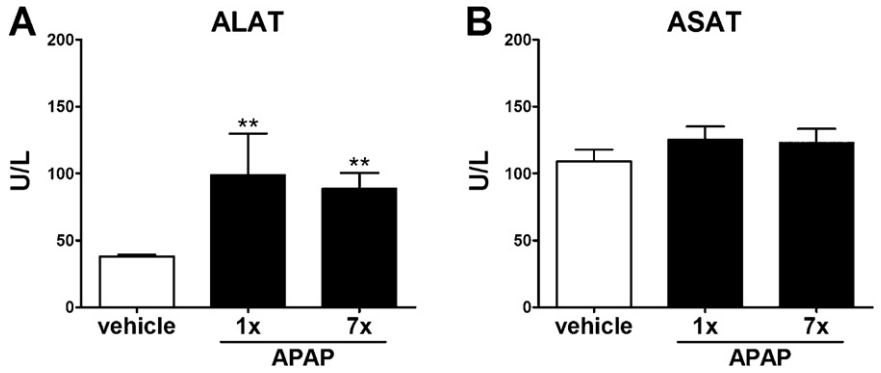

Fig. 6. Serum levels of liver enzymes from animals orally exposed to vehicle or APAP. Mice were orally exposed to a single or seven consecutive doses of vehicle or APAP. Within 24 h of the last oral dosing, serum and plasma was collected and ALAT (A) and ASAT (B) levels in plasma were determined (each bar represents the mean ± SEM of 8–16 (controls) or 3–8 (APAP) animals per group). $^{***}p < 0.001$.

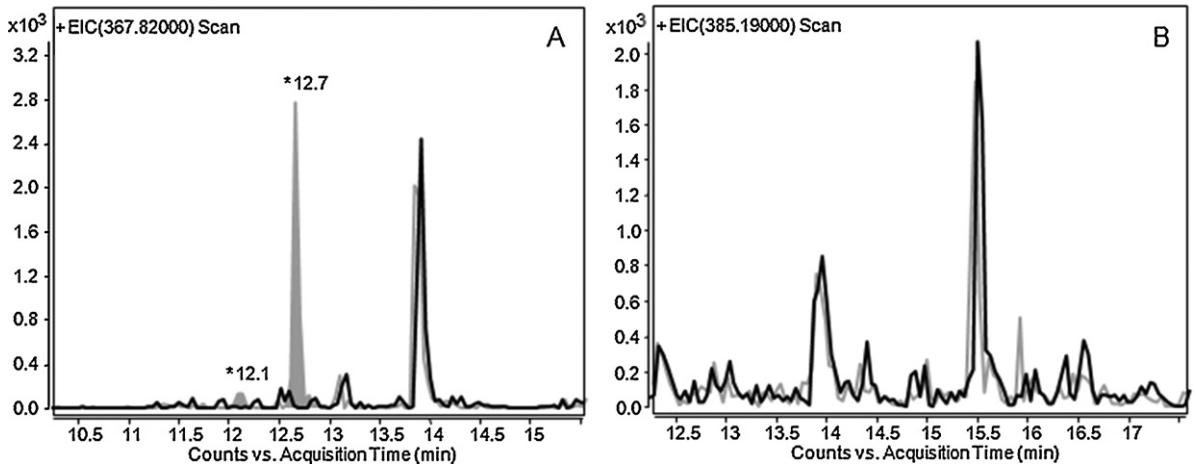

Fig. 7. LC–MS results of a control (black trace) and APAP-dosed (gray trace) serum sample from the mouse study. EIC's of *m*/*z* 367.82 (A) of the triply charged C_{34}(NAPQI)SYDEHAK and *m*/*z* 385.19 (B) representing the doubly charged C_{579}(NAPQI)KDALA peptide.

Table 1
Summary of quantification results.

Calculated MSA values (average ± stdev, $n = 8$)	1 day		7 days	
	APAP	Control	APAP	Control
Total mg MSA/mL serum	69.3 ± 5.3	64.3 ± 8.6	56.3 ± 9.9	47.0 ± 5.0
μM MSA final sample	60.3 ± 5.4	55.8 ± 7.8	57.7 ± 10.8	48.9 ± 5.5
% MSA modified by NAPQI	0.20 ± 0.12	0	0.21 ± 0.09	0
μM NAPQI-MSA final sample	0.12 ± 0.08	0	0.12 ± 0.07	0
nmol NAPQI-MSA/mL serum	2.1 ± 1.4	0	1.8 ± 1.0	0

experiment were found to be 0.20% and 0.21% of the total MSA concentration, respectively, which represents a final sample concentration of NAPQI-MSA in the nanomolar range (Table 1). As expected, the detected adduct levels are extremely low, but, due to the prolonged drug treatment, higher NAPQI-MSA adduct levels were expected in the seven-day experiment. Surprisingly, the detected adduct levels were similar for both mouse experiments, which is in good agreement with the plasma levels of liver enzymes and histological liver analysis. A possible explanation of these results could be adaptation to the drug treatment after prolonged exposure. On the other hand, the liver function may have already been severely disrupted after a single high dose of APAP such that prolonged exposure on seven consecutive days did not lead to the formation of more NAPQI and subsequent NAPQI-MSA adducts than in the one-day experiment.

The average NAPQI-MSA serum concentration was calculated to be 2.1 and 1.8 nmol/mL serum for the one- and seven-day experiment, respectively. These levels are 50 to 700-fold higher than previously detected in patients after APAP overdose [17]. This disagreement may have several causes, such as inter-species differences and the different methods used for quantification. Furthermore, relatively high standard deviations were observed for the NAPQI-MSA adduct levels. These may partly be due to variation caused by the sample preparation and analysis method, but mainly results from the individual biological variation between the eight mice in a treatment group. Similar to humans, each mouse is genetically distinct and a mouse population may display the same variation in response as a human population [38,39]. This was also observed for the current experiment, as reflected by the physiological behavior of the mice as well as the detected NAPQI-MSA levels and standard deviations. On the other hand, great care should always be taken when extrapolating results from *in vitro* experiments to *in vivo* studies and from animal models to the human situation. The difference in covalent drug binding sites *in vitro* and *in vivo*, and between HSA and MSA may not be of any influence on the observed ADRs of the two species, but, when studying the mechanisms behind ADRs, a difference in number and absence or presence of drug binding sites on target proteins involved in human signaling pathways may influence the outcome significantly.

4. Conclusion

The developed analytical strategy was successfully applied to mouse serum samples resulting from a drug exposure study and achieved detection and quantification of low-abundant drug–albumin adducts despite the presence of an excess of non-modified protein. As expected, the NAPQI-MSA adduct levels were extremely low, approximately 0.2% of the total MSA, but, due to the optimized strategy, the NAPQI-MSA concentration in the final samples was still in a detectable range. Additionally, the increased selectivity and sensitivity of the targeted methodology allows for confirmation and characterization of the NAPQI-MSA adduct in terms of localization of the adduct formation site. Another advantage of the examined identification and quantification approach is its generic nature, which permits application to different drug–albumin adducts.

Acknowledgements

The authors acknowledge the technical support provided by Dr. M. Stitzinger and M.H.M. van Tuyl, M.Sc. and the technicians of NOTOX BV ('s-Hertogenbosch, The Netherlands) for measuring liver enzymes. This research was performed within the framework of project D3-201 "Towards novel translational safety biomarkers for adverse drug toxicity" of the Dutch Top Institute Pharma.

References

[1] S.F. Zhou, E. Chan, W. Duan, M. Huang, Y.Z. Chen, Drug Metab. Rev. 37 (2005) 41.
[2] J.V. Castell, M. Castell, Curr. Opin. Allergy Clin. Immunol. 6 (2006) 258.
[3] C. Ju, Toxicol. Pathol. 37 (2009) 12.
[4] M.J. Masson, R.A. Peterson, C.J. Chung, M.L. Graf, L.D. Carpenter, J.L. Ambroso, D.L. Krull, J. Sciarrotta, L.R. Pohl, Chem. Res. Toxicol. 20 (2007) 20.
[5] S. Zhou, J. Chromatogr. B 797 (2003) 63.
[6] K. Ikehata, T.G. Duzhak, N.A. Galeva, T. Ji, Y.M. Koen, R.P. Hanzlik, Chem. Res. Toxicol. 21 (2008) 1432.
[7] Y. Qiu, L.Z. Benet, A.L. Burlingame, J. Biol. Chem. 273 (1998) 17940.
[8] J.S. Landin, S.D. Cohen, E.A. Khairallah, Toxicol. Appl. Pharmacol. 141 (1996) 299.
[9] R.M. Methogo, P.M. Dansette, K. Klarskov, Int. J. Mass Spectrom. 268 (2007) 284.
[10] Y.M. Koen, W. Yue, N.A. Galeva, T.D. Williams, R.P. Hanzlik, Chem. Res. Toxicol. 19 (2006) 1426.
[11] J. Gan, Q. Ruan, B. He, M. Zhu, W.C. Shyu, W.G. Humphreys, Chem. Res. Toxicol. 22 (2009) 690.
[12] J. Ghuman, P.A. Zunszain, I. Petitpas, A.A. Bhattacharya, M. Otagiri, S. Curry, J. Mol. Biol. 353 (2005) 38.
[13] J.L. Moreland, A. Gramada, O.V. Buzko, Q. Zhang, P.E. Bourne, BMC Bioinformatics 6 (2005) 21.
[14] M. Azarkan, J. Huet, D. Baeyens-Volant, Y. Looze, G. Vandenbussche, J. Chromatogr. B 849 (2007) 81.
[15] W.C. Lee, K.H. Lee, Anal. Biochem. 324 (2004) 1.
[16] X.X. Yang, Z.P. Hu, S.Y. Chan, S.F. Zhou, Clin. Chim. Acta 365 (2006) 9.
[17] M.C. Damsten, J.N. Commandeur, A. Fidder, A.G. Hulst, D. Touw, D. Noort, N.P. Vermeulen, Drug Metab. Dispos. 35 (2007) 1408.
[18] D. Noort, A.G. Hulst, R. Jansen, Arch. Toxicol. 76 (2002) 83.
[19] D.C. Evans, A.P. Watt, D.A. Nicoll-Griffith, T.A. Baillie, Chem. Res. Toxicol. 17 (2004) 3.
[20] J.S. Hoos, M.C. Damsten, J.S.B. de Vlieger, J.N.M. Commandeur, N.P.E. Vermeulen, W.M.A. Niessen, H. Lingeman, H. Irth, J. Chromatogr. B 859 (2007) 147.
[21] J.A. Loo, C.G. Edmonds, R.D. Smith, Anal. Chem. 63 (1991) 2488.
[22] M. Otagiri, Drug Metab. Pharmacokinet. 20 (2005) 309.
[23] J.H. Lin, Drug Metab. Dispos. 23 (1995) 1008.
[24] L.M. Kwast, D. Fiechter, I. Hassing, R. Bleumink, L. Boon, I.S. Ludwig, R.H. Pieters, Toxicol. Sci. 121 (2011) 312.
[25] L. Switzar, M. Giera, H. Lingeman, H. Irth, W.M. Niessen, J. Chromatogr. A 1218 (2011) 1715.
[26] P.C. Kelleher, C.J. Smith, R. Pannell, J. Chromatogr. 173 (1979) 415.
[27] E. Gasteiger, A. Gattiker, C. Hoogland, I. Ivanyi, R.D. Appel, A. Bairoch, Nucleic Acids Res. 31 (2003) 3784.
[28] K.J. Bronsema, R. Bischoff, N.C. van de Merbel, J. Chromatogr. B 893–894 (2012) 1.
[29] Q. Huang, X. Jin, E.T. Gaillard, B.L. Knight, F.D. Pack, J.H. Stoltz, S. Jayadev, K.T. Blanchard, Mutat. Res. 549 (2004) 147.
[30] D.J. Jollow, J.R. Mitchell, W.Z. Potter, D.C. Davis, J.R. Gillette, B.B. Brodie, J. Pharmacol. Exp. Ther. 187 (1973) 195.
[31] J.R. Mitchell, D.J. Jollow, W.Z. Potter, D.C. Davis, J.R. Gillette, B.B. Brodie, J. Pharmacol. Exp. Ther. 187 (1973) 185.
[32] R. Singhal, P.E. Ganey, R.A. Roth, J. Pharmacol. Exp. Ther. 341 (2012) 377.
[33] D.E. Amacher, Regul. Toxicol. Pharmacol. 27 (1998) 119.
[34] J. Ozer, M. Ratner, M. Shaw, W. Bailey, S. Schomaker, Toxicology 245 (2008) 194.
[35] K. Yapar, A. Kart, M. Karapehlivan, O. Atakisi, R. Tunca, S. Erginsoy, M. Citil, Exp. Toxicol. Pathol. 59 (2007) 121.
[36] Y.C. Kim, S.J. Lee, Toxicology 128 (1998) 53.
[37] A.J. Singer, T.R. Carracio, H.C. Mofenson, Ann. Emerg. Med. 26 (1995) 49.
[38] M.F. Festing, Crit. Rev. Toxicol. 18 (1987) 1.
[39] R. Lathe, Genes Brain Behav. 3 (2004) 317.